Science of the Total Environment 832 (2022) 155010

Contents lists available at ScienceDirect

Science of the Total Environment

journal homepage: www.elsevier.com/locate/scitotenv

Effects of heavy grazing on the microclimate of a humid grassland mountain ecosystem: Insights from a biomass removal experiment

Paola Montenegro-Díaz [a,*], Rolando Célleri Alvear [a,b], Bradford P. Wilcox [c], Galo Carrillo-Rojas [a,d]

[a] Departamento de Recursos Hídricos y Ciencias Ambientales, Universidad de Cuenca, Cuenca, Ecuador
[b] Facultad de Ingeniería, Universidad de Cuenca, Cuenca, Ecuador
[c] Department of Ecology and Conservation Biology, Texas A&M University, College Station, TX, USA
[d] Facultad de Ciencias Químicas, Universidad de Cuenca, Cuenca, Ecuador

HIGHLIGHTS

- A biomass removal experiment simulates an overgrazing in Andean grassland (páramo).
- The removal increased the albedo, upward longwave energy, and surface temperature.
- These variables and the grass returned to their historical values after 1.75 years.
- During the recovery period, a cooling feedback was observed.
- Daily albedo may be a suitable indicator of grassland health in the páramo.

GRAPHICAL ABSTRACT

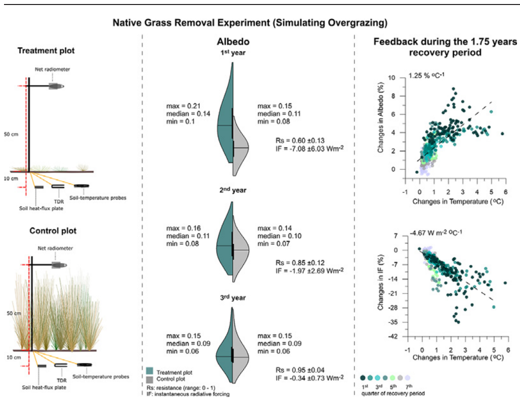

ARTICLE INFO

Editor: Anastasia Paschalidou

Keywords:
Fast feedback
Warming forces
Ecosystem resistance
Restoration
Ecosystem stability

ABSTRACT

In high-altitude Andean grasslands (páramo), overgrazing leads to alterations in both vegetation and microclimate. These alterations need to be identified to devise land management strategies that will preserve and enhance ecosystem processes. To elucidate this issue, we designed an overgrazing experiment: we selected two plots covered with native grass (pajonal), in one of which we mowed to the ground surface. We left the second plot undisturbed to serve as a control. For both plots, we continuously monitored albedo and ancillary energetic components to generate quarterly and yearly comparisons for the following parameters: (a) impacts on albedo and resilience of grass; (b) radiative forcing of albedo; and (c) land surface temperature feedback during the recovery period. In the first quarter following removal, when the soil was covered with light litter, median albedo increased 38.81% (0.16 ± 0.02), then began a gradual decrease, which continued until its full recovery 1.75 years later (0.10 ± 0.01). During the first year of the experiment, a strong mean negative instantaneous radiative forcing was observed (-7.08 ± 6.03 Wm^{-2}), signifying a reduction in net shortwave energy. This forcing returned to normal, pre-intervention conditions (-0.55 ± 0.97 Wm^{-2}) after 1.75 years, equal to the energetic recovery period of the grass. Both the amount (from 133.0 ± 44.72 to 119.67 ± 39.30 Wm^{-2}) and the partitioning (net shortwave decreased 5%; net longwave increased 9.7%) of net energy were altered after removal, evidence of cooling feedback during the recovery period. This feedback indicated that the decrease in albedo (1.25%) or instantaneous radiative forcing (-4.67 Wm^{-2}) resulted in a decrease in land surface temperature of 1 °C. Thus, our overgrazing experiment without soil destruction followed by a natural recovery time has identified the energetic recovery period for grass in the páramos; suggesting the albedo as a good indicator of grass resilience.

* Corresponding author at: Universidad de Cuenca, Cuenca 010207, Ecuador.
E-mail addresses: paola.montenegro@ucuenca.edu.ec (P. Montenegro-Díaz), rolando.celleri@ucuenca.edu.ec (R.C. Alvear), bwilcox@tamu.edu (B.P. Wilcox), galo.carrillo@ucuenca.edu.ec (G. Carrillo-Rojas).

http://dx.doi.org/10.1016/j.scitotenv.2022.155010
Received 19 January 2022; Received in revised form 29 March 2022; Accepted 30 March 2022
Available online 2 April 2022

1. Introduction

Shortwave albedo characterizes the surfaces' ability to reflect shortwave energy. Quantification of albedo is essential for understanding micro, local, regional, and global climate because it is part of the land surface and atmosphere balances that regulate all environmental processes (evapotranspiration, carbon exchange, etc.) (Bramer et al., 2018; IPCC, 2018). When human activities transform the land, albedo is modified—which creates a radiative forcing (or warming forcing) that interrupts the energy exchange between the land surface and atmosphere (Sagan et al., 1979; Wang et al., 2019). This altered energy exchange may cause warming and cooling feedbacks by altering the land surface temperature (Xiao et al., 2017) depending on latitude, land use, vegetation phenology, and soil stage (e.g., Arora and Montenegro, 2011; Claussen et al., 2001; Findell et al., 2007).

Albedo is potentially modified by grazing through vegetation change, green leaf consumption, and land trampling. Such short-term modifications in albedo, lead to instantaneous changes in the radiative forcing, feedbacks, and microclimate—that may influence the regional climate (Dickinson and Hanson, 1979). It is also known that grazing-induced effects on albedo vary across ecosystems (te Beest et al., 2016; Wang et al., 2019; Zhao et al., 2017). All these characteristics make albedo a good biophysical indicator (Zheng et al., 2019) to measure the vegetation stage and energy availability. Nevertheless, we are unaware of any study that has assessed how grazing affects albedo in tropical mountain regions.

Páramo ecosystems occupy some 45,425 km^2 of the highlands of Latin America, the largest extent being found in Colombia and Ecuador and discontinuous patches in Costa Rica (Cerro Chirripó), Venezuela (Páramos de Mérida) and northern Peru (Carrillo-Rojas, 2019; Correa et al., 2020). These ecosystems are characterized by perennial native grasslands, dark, humid volcanic soils, a humid climate, and year-round sustained water flow (Mosquera et al., 2015). Because of these characteristics, páramo ecosystems have been used since the pre-Inca period for grazing of camelids (llama, alpaca, and vicuña), sheep, and cattle (Postigo, 2014). It is known that grazing can alter the properties of grass and soils, as well as soil moisture dynamics and water yields, to a greater or lesser extent depending on the grazing intensity (Fernandez Monteiro et al., 2011; Hofstede, 1995; Marín et al., 2018; Montenegro-Díaz et al., 2019; Podwojewski et al., 2006). It is also known that grazing modulates the albedo and feedbacks of mountain ecosystems—e.g., cooling in tundra ecosystems (te Beest et al., 2016)—but the extent and duration of grazing impacts on albedo, instantaneous radiative forcing, and feedbacks in páramo ecosystems have not yet been studied. Hence, these processes and the resilience of these ecosystems have not yet been quantified when such variables are focused on the ability to resist and to recover (Ingrisch and Bahn, 2018) from the grazing. As we can see, páramo ecosystems are the main source of water for households and the main source of income for indigenous people and farmers living in their highlands and valleys. Consequently, evidence-based land management, including strategies for ecosystem restoration, is essential for preserving these ecosystems and their services; there is an urgent need to undertake such studies.

Grazing may alter the energy balance, therefore it is important to quantify the effects of overgrazing on the energy components of the environment. Consequently, we hypothesize that overgrazing in páramo ecosystems increases the albedo via changes in the land surface reflectivity and then, produces a radiative forcing that alters the energy available for environmental processes. For this reason, we designed an experiment that would simulate overgrazing (by biomass removal) to quantify (a) impacts on albedo and resilience of grass; (b) instantaneous radiative forcing of albedo; and (c) land surface temperature feedback during albedo recovery period.

2. Study area

The Zhurucay Ecohydrological Observatory (hereafter Zhurucay), shown in Fig. 1a-b, is located within a wet páramo ecosystem in southern Ecuador, on the western side of the Andes Highlands. Zhurucay is adjacent to the Quimsacocha National Recreation Area (MAATE, 2015), an undisturbed catchment of 7.5 km^2 that ranges in elevation from 3400 to 3900 m a.s.l (slopes from 0.0 to 40%) and has high biodiversity and endemism with a low livestock rate (<0.1 animals ha^{-1}). Like all wet páramo ecosystems, the Zhurucay is a strategic source of water (SENPLADES, 2017) and a prime carbon storage zone (Carrillo-Rojas et al., 2019). These attributes make the Zhurucay an ideal place for investigating the hydrological, meteorological, and ecological processes of páramo ecosystems (e.g., Carrillo-Rojas et al., 2020; Lazo et al., 2019; Ochoa-Sánchez et al., 2020).

The Zhurucay exhibits only a slight thermal seasonality. The micrometeorological record from January 2015 to December 2019 showed an annual average air temperature of 6.32 $\pm$ 0.55 °C, average annual relative humidity of 94.04 $\pm$ 0.79%, and average annual shortwave energy of 288.67 $\pm$ 21.12 Wm^{-2}. Precipitation is bimodal with unmarked dry seasons—similar to the pattern seen in other páramo ecosystems of the region (Celleri et al., 2007)—and fog and drizzle are present almost daily (Padrón et al., 2015). Average annual precipitation is 1345 mm (Sucozhañay and Célleri, 2018) and average annual drizzle amounts to 340.1 mm (Berrones et al., 2021). Annual actual evapotranspiration averages 634.7 $\pm$ 9.0 mm (Carrillo-Rojas et al., 2019). The native vegetation consists mostly (>80%) of C3 tussock grass, *Calamagrostis* sp. locally known as "pajonal," and interspersed patches of cushion plants and forest *Polylepis* sp. No non-native species have invaded the observatory. The dominant soil type is Andosol (75%), the remainder being Histosols (according to the US soil taxonomy); the surface soils of both types are rich in organic matter (Mosquera et al., 2015).

The Zhurucay encompasses one of the most complete super-sites for ecohydrological and meteorological monitoring in the Andean region, detailed in Carrillo-Rojas et al. (2019) and Sucozhañay and Célleri (2018). This super-site enables not only conventional measurement of weather, topography, soil taxonomy, and vegetation species within the observatory, but also monitoring of the energy and water fluxes of the land surface and atmosphere (Ochoa-Sánchez et al., 2020). The instrumented hillslope of the super-site, which covers 392 m^2 (23 m long x 17 m wide with a slope of 20%), is surrounded by a fence that prevents intrusion by humans, herbivory, or grazing (it does not prevent rodents nor invertebrates). The hillslope is covered with perennial tussock grass (*Calamagrostis* sp.) without exposure of bare soil; this grass is dark brownish-green in color and about 0.50 m in mean height, with a great amount of standing dead biomass. The grass roots generally penetrate the soil to a depth of 0.10–0.20 m. The Andosol soils have a mean depth of 0.43 m, an organic matter content of 57.41%, and a water retention capacity of 0.72 cm^3 cm^{-3} (saturation point = 0.5 cm^3 cm^{-3}, wilting point = 0.8 cm^3 cm^{-3}).

3. Methods

3.1. Study design and experimental setup

Within the instrumented hillslope of the super-site, at an inclination of <8°, we delineated two parallel plots measuring 195.5 m^2 each (23 m long x 8.5 m wide) for energy flux and soil moisture monitoring: a Treatment plot and a Control plot. A set of sensors were permanently installed in the middle of each plot (in November 2014) to avoid overlap of the sensors' footprints (each footprint having a radius of 3.0 m, distance between the set of sensors was 11 m). Each set of sensors consisted of a net radiometer installed to a height of 0.50 m above the soil surface, with a heat flux plate and a time domain reflectometer installed in the soil at a depth of 0.10 m (see Fig. 1b and Appendix A, which details the main characteristics of the set of sensors). This paired design enables comparison of micrometeorological variables under grazed versus undisturbed conditions.

On August 10, 2016 we began our study of the effects of overgrazing—a traditional practice in páramo ecosystems—on microclimate. Using a lawnmower, we removed the grass to the soil surface in Treatment plot. The grass shoots were not removed. Vegetation removal was done in a dry month (August, for which precipitation data covering the previous five years showed a range of 24.5–62.7 mm month^{-1}). We maintained

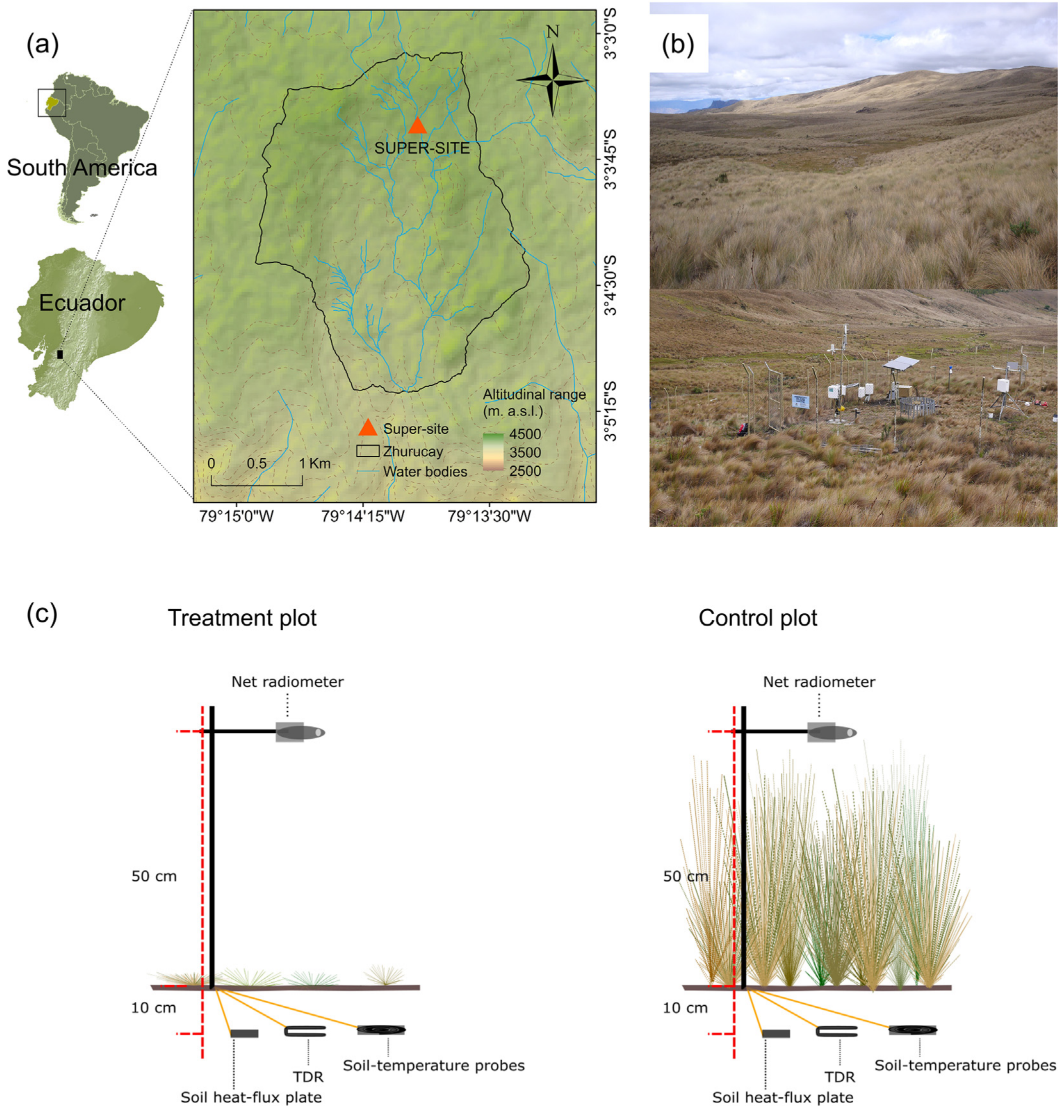

Fig. 1. Study area and design of overgrazing experiment. (a-b) Geographic location and views of the Zhurucay Ecohydrological Observatory basin and the super-site for ecohydrological and meteorological monitoring; (c) Arrangement of sensors for the Treatment and Control plots.

the plot free of any other disturbances and allowed the grass to regenerate passively (natural restoration). The photos in Fig. 2 compare the Treatment plot with Control plot (reference plot) at three intervals: one month, six months, and three years after vegetation removal. Further details on the design of the overgrazing experiment and restoration strategy may be found in Appendix B.

3.2. Data treatment and statistical analysis

The data were recorded as a 4.8-year dataset (January 1, 2015–August 9, 2019). We used five-minute time series plots to identify noise and outliers in the dataset and removed the few doubtful values detected (<2.0%), obviating the need for data gap filling. Although not incorporated into the analysis, the grass regrowth was measured biweekly inside six subplots within Treatment plot after the grass removal, during the overgrazing experiment. A photographic record and measurements of grass regrowth may be found in Appendix C.

Our analysis was based on daily data recorded in Treatment and Control plots during two periods: (1) the 1.8-year period preceding the overgrazing experiment, when the land cover of both plots was still in its natural, undisturbed state; and (2) the 3-year period during which the overgrazing experiment was conducted in Treatment plot. To enhance the robustness of our interpretations, we divided the second period into (a) one-year sub-periods (to correspond with previous studies of land use change) and (b) ¼-year sub-periods (to have sub-periods short enough that surface optical properties/reflectivity do not change dramatically—i.e., from bare soil to complete grass regrowth—or too slowly.)

3.2.1. Quantifying the impacts on albedo and resilience of grass

To analyze differences in albedo between Treatment plot and Control plot before and during the overgrazing experiment, we first used the non-parametric Mann–Whitney test (H_0: no difference between Treatment and Control plots observed). Second, we quantified the impacts of the overgrazing experiment on albedo using RStudio software HydroGOF package functions to inform about how larger or shorter was Treatment plot from Control plot in percentage ($MD_{\%}$), mean absolute difference (MAD), root mean square difference (RMSD), and the linear correlation (Pearson correlation [r]). Third, we quantified the resilience that includes the resistance of grass to change after the removal and the recovery of grass from the removal (according to Capdevila et al. (2020) and Ingrisch and Bahn (2018)) —through albedo as a representative variable. Resistance index (Rs, proposed by Orwin and Wardle (2004)) measures the ability of disturbed grass (i.e., Treatment plot) to withstand the effects of the overgrazing experiment. The index used the albedos (α) of Control and

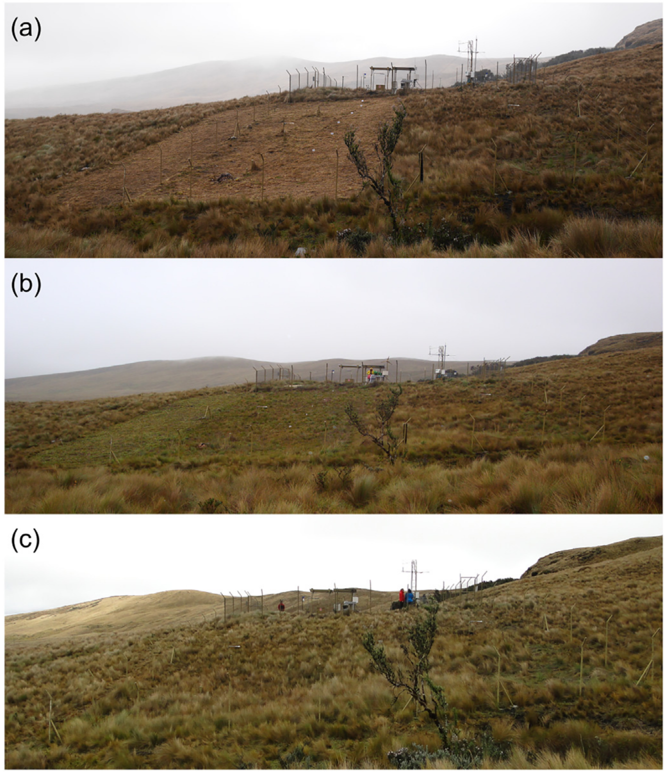

Fig. 2. Views of Treatment plot (left) and Control plot (right) at (a) one month, (b) six months, and (c) three years after the biomass removal.

Treatment plots before and during the overgrazing experiment (Eq. (1)); the values were bounded by +1 and 0, with +1 meaning no change was caused by the overgrazing experiment, and 0 a complete disturbance. The period of recovery from the grass removal was the time when the albedo of Treatment plot (as measured by all the aforementioned metrics [$MD_{\%}$, MAD, RMSD, r, Rs]) recovered to its pre-experiment levels.

$$\mathrm{Rs} = \left(2\left|\alpha_{\mathrm{Control\ plot}} - \alpha_{\mathrm{Treatment\ plot}}\right|\right)\left(\alpha_{\mathrm{Control\ plot}} + \left|\alpha_{\mathrm{Control\ plot}} - \alpha_{\mathrm{Treatment\ plot}}\right|\right)^{-1} \quad (1)$$

3.2.2. Quantifying the radiative forcing of albedo

Instantaneous radiative forcing (IF_α) describes the instantaneous influence of a change in albedo over shortwave energy budget (Bozzi et al., 2015; Xiao et al., 2017). It was calculated to characterize microclimatic responses (at a land surface level of 0.5 m) to the overgrazing experiment. This calculation (Eq. (2)) was based on the downward shortwave energy (S_{down}), the difference between the albedos of Treatment and Control plots, the fraction of Earth's surface affected by the albedo change (f_E = 1 when the entire Treatment plot was affected), and the fraction of downward shortwave energy that retained the top of the atmosphere (t_a) (Bozzi et al., 2015). The latter is a proxy of the clearness index (K_T), which is the fraction of extraterrestrial energy (S_o) that reaches the Earth's surface ($K_T = S_{down}\,S_o^{-1}$) (Bozzi et al., 2015).

$$IF_\alpha = -S_{down}\left(\alpha_{\mathrm{Treatment\ plot}} - \alpha_{\mathrm{Control\ plot}}\right) f_E\, t_a \quad (2)$$

3.2.3. Quantifying the feedback of albedo

To identify the contribution of the grazing experiment to microclimatic dynamics, we estimated the magnitude of the fast (daily scale) feedback (γ), through (1) the linear regression slope of the changes in albedo (Δ_α, as a percentage) versus those in estimated land surface temperature (ΔT_s), following the method of Fletcher et al. (2015); and (2) the linear regression slope of the changes in instantaneous radiative forcing (ΔIF_α) versus those in estimated land surface temperature (ΔT_s), following the method of Xiao et al. (2017). The changes were obtained in the form Treatment versus Control plot during the recovery period of grass. We used the Stefan-Boltzmann law to estimate land surface temperatures in Treatment versus Control plot (described in Appendix D) (Nighttime microclimatic effects were not analyzed because shortwave energy does not exist at night.)

4. Results

4.1. Impacts on albedo and resilience of grass

Under undisturbed conditions, Treatment and Control plots had the same median albedo (0.11 ± 0.01; p.value >0.05), as illustrated in Fig. 3. The disturbance-free condition of the two plots—reflected by the null impacts on albedo using the metrics: percentage mean difference ($MD_{\%}$), mean absolute difference (MAD), root mean square difference (RMSD), and Pearson correlation (r), and the complete resistance of grass reflected by resistance index (Rs) shown in Table 1 and Fig. 4—offered an optimal environment for the grass to maintain its steady state ($MD_{\%}$ = 0.00%; MAD = 0.00; RMSD = 0; r = 0.99; Rs = 0.97 ± 0.03).

Fig. 3 shows the albedo values of Treatment and Control plots during the three years of the overgrazing experiment following the grass removal in Treatment plot. The quarterly and annual analyses show a decreasing trend for the effects of simulated overgrazing on albedo (that is, 1st year >2nd year >3rd year), but an increasing trend for grass resistance (that is, 1st year <2nd year <3rd year), as shown in Table 1 and Fig. 4. The maximal impact and minimal resistance were found in the first year of the experiment ($MD_{\%}$ = 26.32%; MAD = 0.03; RMSD = 0.03; r = 0.83; Rs = 0.60 ± 0.13), peaking in the 1st quarter ($MD_{\%}$ = 38.81%; MAD = 0.05; RMSD = 0.05; r = 0.84; Rs = 0.45 ± 0.11) where albedo strongly increased (Treatment median = 0.16 ± 0.02; Control median = 0.12 ± 0.01). In the second year, impact and resistance were both noticeably altered until the 2nd quarter ($MD_{\%}$ = 11.54%; MAD = 0.01; RMSD = 0.01; r = 0.87; Rs = 0.80 ± 0.10) after which no further changes occurred through the end of the third year ($MD_{\%}$ ≤ 2.43%; MAD = 0.00; RMSD = 0.00; r ≥ 0.94; Rs ≥ 0.93 ± 0.04; p.value >0.05). In other words, with a strategy of natural regeneration, grass recovered undisturbed reflectivity conditions (Treatment median = 0.10 ± 0.01; Control median = 0.10 ± 0.01) 1.75 years after the start of the overgrazing experiment.

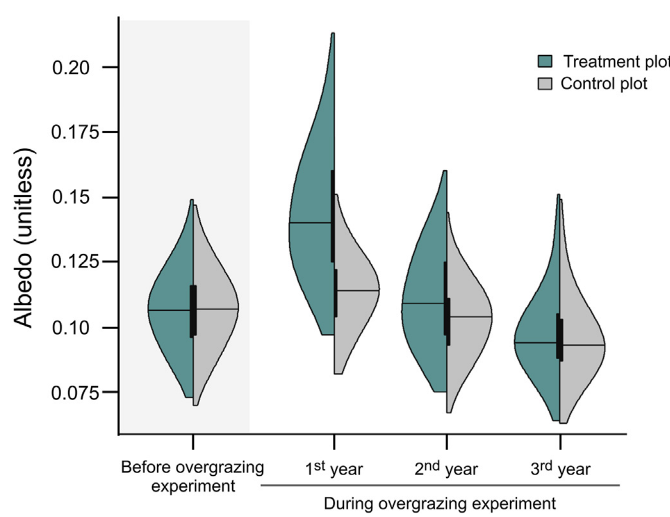

Fig. 3. Comparison of albedo in Treatment and Control plots before and during the overgrazing experiment. Each violin plot indicates the distribution, median (horizontal line), quartiles (vertical black bars), and maximum and minimum (violin limits) albedos.

Table 1
Impacts on albedo, resistance of grass, and instantaneous radiative forcing preceding and during the overgrazing experiment (for each of the three years and for each quarter).

Periods	Impacts				Resistance		Instantaneous radiative forcing	
	$MD_{\%}$ (%)	MAD (−)	RMSD (−)	r (−)	MEAN (−)	SD (−)	MEAN (W m^{-2})	SD (W m^{-2})
Preceding the experiment*	0.15	0.00	0.00	0.99	0.97	±0.03	0.03	±0.43
During the experiment								
First year	26.32	0.03	0.03	0.83	0.60	±0.13	−7.08	±6.03
1st quarter	38.81	0.05	0.05	0.84	0.45	±0.11	−11.85	±7.53
2nd quarter	27.39	0.03	0.03	0.91	0.58	±0.08	−7.83	±4.84
3rd quarter	18.70	0.02	0.02	0.92	0.69	±0.06	−3.86	±1.90
4th quarter	19.37	0.02	0.02	0.89	0.68	±0.11	−4.63	±4.76
Second year	8.02	0.01	0.01	0.89	0.85	±0.12	−1.97	±2.69
1st quarter	16.19	0.02	0.02	0.91	0.73	±0.10	−4.08	±3.32
2nd quarter	11.54	0.01	0.01	0.87	0.80	±0.10	−3.01	±2.46
3rd quarter*	2.43	0.00	0.00	0.94	0.94	±0.05	−0.55	±0.97
4th quarter*	0.78	0.00	0.00	0.98	0.95	±0.03	−0.18	±0.53
Third year*	1.64	0.00	0.00	0.98	0.95	±0.04	−0.34	±0.73
1st quarter*	2.30	0.00	0.00	0.95	0.93	±0.04	−0.53	±1.08
2nd quarter*	1.49	0.00	0.00	0.99	0.95	±0.04	−0.34	±0.69
3rd quarter*	1.63	0.00	0.00	0.99	0.96	±0.03	−0.28	±0.36
4th quarter*	1.04	0.00	0.00	0.99	0.95	±0.03	−0.17	±0.46

* Indicates that the data from both plots are statistically significant (p.value >0.05). Percentage mean difference ($MD_{\%}$), mean absolute difference (MAD), root mean square difference (RMSD), Pearson correlation (r), and standard deviation (SD).

4.2. Instantaneous radiative forcing of albedo

The microclimate's response to the overgrazing experiment is expressed through the instantaneous radiative forcing (IFα). Under the undisturbed conditions, there was no instantaneous radiative forcing at land surface level (IF_{α} = 0.03 ± 0.43 Wm^{-2})—but this situation changed after the grass was removed. The albedo changed, which created an instantaneous radiative forcing that steadily increased from negative values (IF_{α} max. = −35.02 Wm^{-2}) to almost zero as can be seen in Table 1 and Fig. 4. The stronger instantaneous radiative forcing was observed in the first year of the overgrazing experiment (IF_{α} = −7.08 ± 6.03 Wm^{-2}), especially in the 1st and 2nd quarters (IF_{α} = −11.85 ± 7.53 Wm^{-2} and -7.83 ± 4.84 Wm^{-2}, respectively). Then, in the second year, a large difference was observed as the natural recovery of the grass decreased the instantaneous radiative forcing (IF_{α} = −1.97 ± 2.69 Wm^{-2})—which was particularly noticeable in the 2nd quarter (IF_{α} = −3.01 ± 2.46 Wm^{-2}). After this point, the instantaneous radiative forcing remained below zero until the end of the third year ($IF_{\alpha} \geq$ −0.55 ± 0.97 Wm^{-2}), evidence of an energetic recovery.

4.3. Feedback of albedo

In our analysis of the fast feedbacks that took place during the 1.75-year energetic recovery period—which is a portion of the overgrazing experiment time (see Sections 4.1 and 4.2)—the magnitude of feedbacks caused by the grass removal was estimated via linear regression slopes. A plot of the feedback from the changes in albedo versus those in estimated land surface temperature (daytime) (Fig. 5a) shows that when albedo decreased 1.25% during the energetic recovery period, the land surface temperature decreased 1 °C. An equal decrease in the land surface temperature was observed when net shortwave energy decreased −4.67 Wm^{-2} during the energetic recovery period (Fig. 5b). This means that the grass removal increased the land surface temperature, and then, it was decreasing to the pre-experimental conditions following the grass recovering.

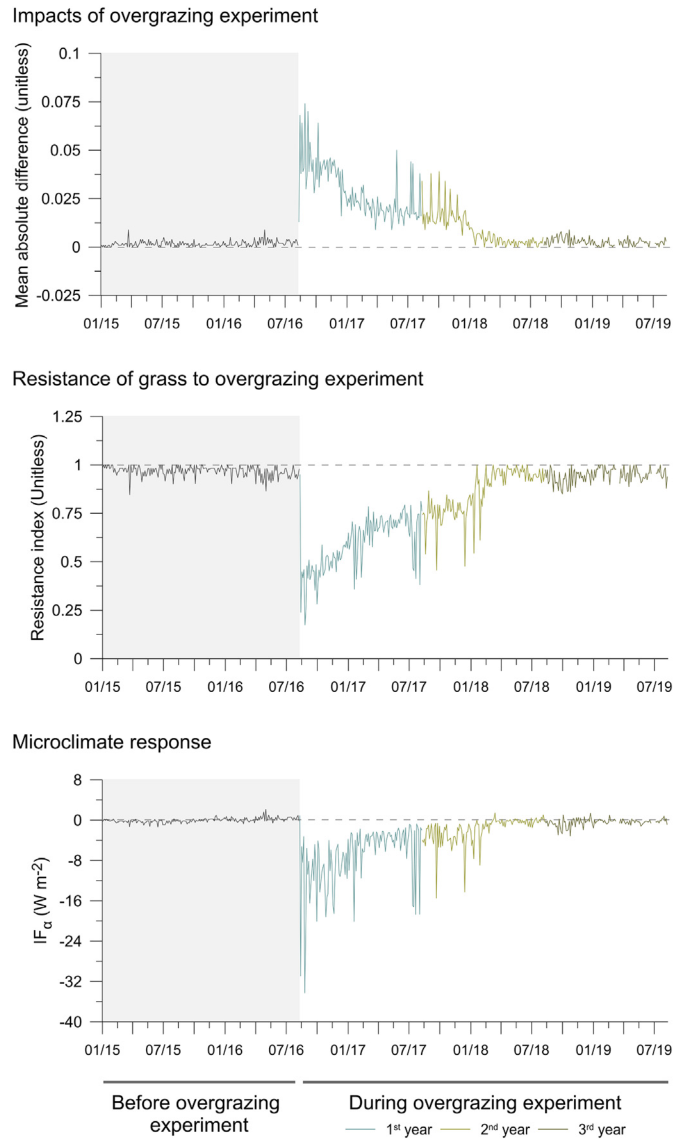

Fig. 4. Time series showing the impacts of overgrazing experiment by mean absolute difference and the resistance of grass by resistance index before and during the overgrazing experiment. The response of the microclimate is reflected by changes in instantaneous radiative forcing (IF_{α}) before and during the overgrazing experiment. (We used a stepping factor every three data points for better visualization.)

5. Discussion

5.1. Impacts on albedo and resilience of grass

Previous studies showing an increase in albedo caused by overgrazing include Gong Li et al. (2000) (with sheep in a Mongolian grassland); te Beest et al. (2016) (after intensive herbivory with reindeer in a Norway shrubland); and Rosset et al. (2001) (after grazing was abandoned in a Swiss sub-alpine grassland). Our overgrazing experiment in the Zhurucay, designed to quantify changes in albedo in a páramo ecosystem during an overgrazing experiment (from an undisturbed to disturbed state to complete recovery), adds to the existing knowledge base. All the metrics tested (i.e., $MD_{\%}$, MAD, RMSD, r) showed a strong increase in albedo in the experimental plot just after the grass was removed (Treatment max. = 0.21 vs Control max. = 0.15), when the dark, humid soil was covered by light litter (residue from the grass removal). Albedo remained high during the first year of the overgrazing experiment (Treatment median = 0.14 ± 0.02 vs Control median = 0.11 ± 0.01), when light litter and green grass were

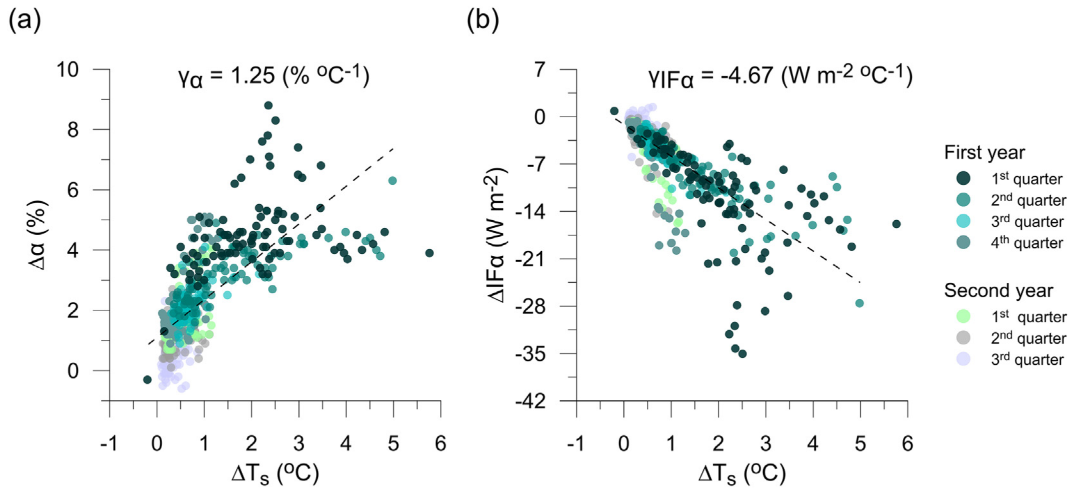

Fig. 5. Quarterly fast feedbacks (γ) during the energetic recovery period of grass: (a) Changes in albedo (Δ_α) versus changes in land surface temperature (ΔT_s); and (b) Changes in instantaneous radiative forcing (ΔIF_α) versus changes in land surface temperature (ΔT_s). The slope of each plot represents the magnitude of the feedback.

dominant (Fig. 2a and b; Appendix C), along with killed by the high insolation recorded, mainly in the 1st quarter (S_{down} median = 421.53 Wm^{-2}). Our experiment using simulated overgrazing exactly replicated the conditions of grazing and natural grass recovery in páramo ecosystems: overgrazing by herbivores exposes grass meristems to freezing and high insolation (Hofstede, 1995; Podwojewski et al., 2006)—which, according to Rosset et al. (2001), delays recovery of the long-term reflectivity of grass. In our study, the gradual recovery of albedo lasted 1.75 year (Treatment median = 0.10 ± 0.01; Control median = 0.10 ± 0.01), and meant that under natural conditions, grass recovery after overgrazing would have taken the same amount of time. However, if other factors that can strongly impact grass cover—such as wildfires, agricultural burning, land trampling, and historical land use—were taken into consideration, the recovery of the grass could be longer or an alternative state might be reached (e.g., bare soil and presence of invasive species).

Resilience is measured quantitatively with a set of proposed indexes (e.g., Ingrisch and Bahn, 2018; Orwin and Wardle, 2004) that work with variables that represent the state of a system (Teng et al., 2020). Albedo is a state variable that indicates the phenology/maturity/health of vegetation and the state of the soil (through changes in the reflectivity) at different spatial and temporal scales—by using ground-based sensors or remote sensing. In our study, albedo effectively informed about the resilience of Andean grasslands, in agreement with findings from other ecosystems worldwide (e.g., Gong Li et al., 2000; Lukeš et al., 2016). Nevertheless, variables such as vegetation coverage, plant diversity, vegetation indexes, and soil properties also measure resilience (e.g., Chou et al., 2020; Gang et al., 2020; Guillaume et al., 2016). We suggest testing these variables to measure resilience in páramo ecosystems.

5.2. Instantaneous radiative forcing of albedo

Satellite and ground-level instantaneous radiative forcing data are used to study land use change at large scales (e.g., Barnes and Roy, 2008) or to develop technologies for mitigating climate change at small spatial scales (Bozzi et al., 2015; VanCuren, 2012). However, instantaneous radiative forcing data are not generally recorded at high temporal resolution, to take into account covariations of shortwave energy and albedo (Bright et al., 2015)—as is needed, for example, to better understand how microclimate is influenced by the phenological transitions of vegetation (from development to senescence) (Richardson et al., 2013). Our study, the first to look at microclimatic responses to overgrazing in páramo ecosystems, had the advantage that daily ground-level radiative forcing data are available.

In the absence of disturbance, instantaneous radiative forcing was close to zero (IFα mean = 0.03 ± 0.43 Wm^{-2}), owing to the slight annual seasonality of downward shortwave energy (Carrillo-Rojas et al., 2016) and the constant reflectivity of brownish-green perennial grass that together produce a steady albedo and net shortwave energy year-round. This steady-state was altered by the overgrazing experiment, which triggered an instantaneous radiative forcing (IFα mean = −7.08 ± 6.03 Wm^{-2}) that decreased net shortwave energy availability in Treatment plot (Treatment mean = 304.40 ± 125.37 Wm^{-2} vs Control mean = 314.34 ± 131.35 Wm^{-2}), especially during the first year. This decrease was associated with the higher amount of energy (upward shortwave energy) reflected from the land surface (Treatment mean = 49.94 ± 25.21 Wm^{-2} vs Control mean = 39.39 ± 18.64 Wm^{-2}) due to the higher reflectivity of light litter and green grass.

Radiative forcing measures the extent to which changes in albedo influence climate warming (or cooling) (Betts, 2001), but it does not take into account non-radiative processes that modify the land surface temperature (Pielke et al., 2002). Hence, this measure by itself can misrepresent the effects of land use change on surface temperature (Davin et al., 2007; Pielke et al., 2002) and must be combined with other measures. To fill this knowledge gap, we quantified the effects of the overgrazing experiment on land surface temperature through feedbacks (Sections 4.3 and 5.3).

5.3. Feedback of albedo

As pointed out by de Wit et al. (2014), the influence of feedbacks from vegetation change on microclimate dynamics are not typically measured and included in scenarios of climate change. In an attempt to fill this knowledge gap, we documented the importance of conserving native grasses for the microclimate of páramo ecosystems. During the 1.75-year recovery time, we measured feedbacks influencing the response of estimated land surface temperature (daytime) to changes in albedo and net shortwave energy. Interestingly, for the Zhurucay, increases in albedo correlate with higher land surface temperatures (at the plot scale), whereas previous studies using satellite data at larger spatio-temporal scales found an inverse correlation between land surface temperature and albedo (e.g., de Wit et al., 2014; VanCuren, 2012; Xiao et al., 2017).

In our study, mostly in the 1st quarter of the recovery period, the higher land surface temperature in Treatment plot (Treatment mean = 7.70 ± 2.34 °C vs Control mean = 6.36 ± 1.7 °C) resulted from the higher availability of upward longwave energy (non-radiative flux) (Treatment mean = 345.77 ± 11.54 Wm^{-2} vs Control mean = 339.15 ± 8.22 Wm^{-2}), which in turn resulted in differences in net energy amount (Treatment mean = 119.67 ± 39.30 Wm^{-2} vs Control mean = 133.0 ± 44.72 Wm^{-2}) and partitioning (Bowen ratio) of net shortwave energy in 5% (Treatment mean = 345.91 ± 130.81 vs Control mean = 363.20 ± 138.67 t Wm^{-2}) and of net longwave energy in 9.7% (Treatment mean = −49.34 ± 27.21 Wm^{-2} vs Control mean = −44.54 ± 25.45)

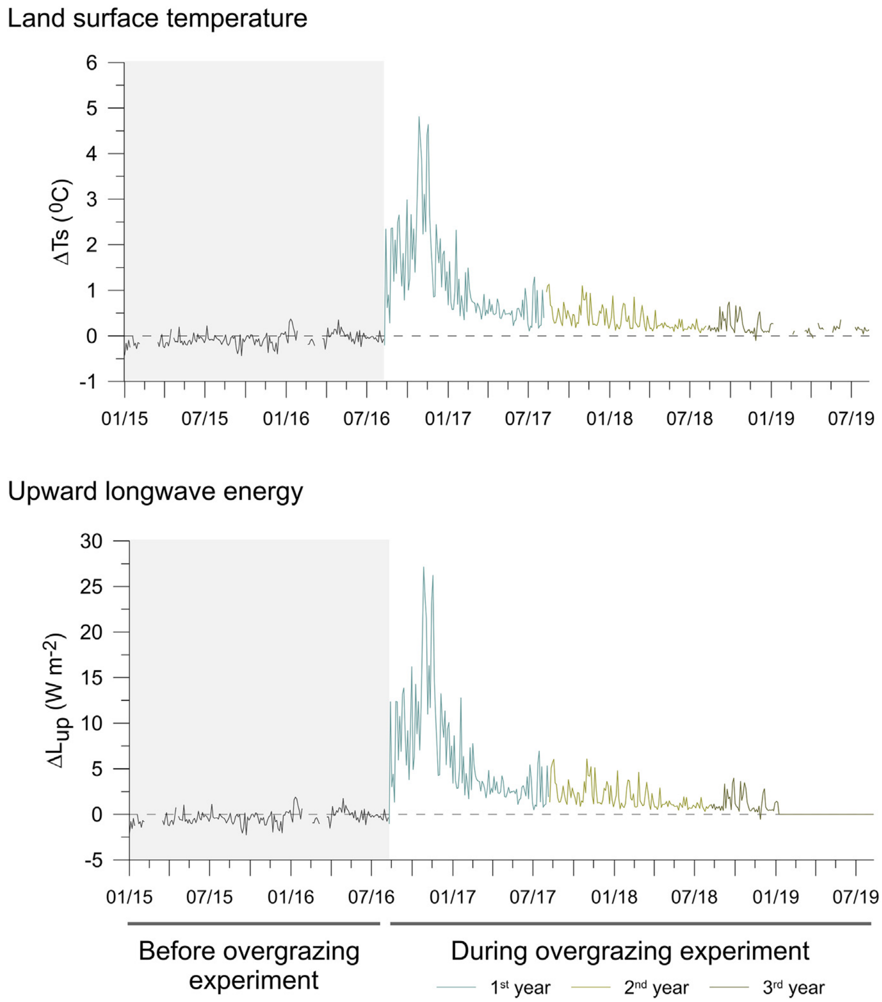

Fig. 6. Time series showing changes in land surface temperature (ΔT_s) and in upward longwave energy (ΔL_{up}) before and during the overgrazing experiment. (We used a stepping factor every three data points for better visualization.)

after the grass removal. To confirm this, we recorded changes in upward longwave energy and in land surface temperature for Treatment plot and compared them with those in Control plot before and during the overgrazing experiment. As shown in Fig. 6, after an initial increase, land surface temperature decreased and continued to decrease as long as the upward longwave energy decreased, until recovery of undisturbed conditions.

6. Conclusions

The aim of our research was to gain, for the first time, insights into how grazing impacts microclimate in the páramos and the resilience (resistance and recovery period) of grass to grazing. During the overgrazing experiment, the energy available for environmental processes was gradually changing. After the grass removal, the albedo, upward longwave energy, land surface temperature increased while the net shortwave energy decreased, then they returned to their historical values 1.75 years later. This recovery period means that our overgrazing experiment did not cross the self-recovery threshold of grass (i.e., the grass did not reach any other alternative state). It was due to the resilience of our grass free of earlier disturbances. Considering our findings, we can reject the hypothesis, which stated that overgrazing in páramo ecosystems increases the albedo via changes in the land surface reflectivity and then, produces a radiative forcing that alters the energy available for environmental processes.

However, we expect that for páramo ecosystems under continued grazing or subjected to practices such as burning, tillage, vegetation change, and soil destruction, the resilience of grass will be lower, and the recovery period will be longer.

Based on our outcomes, albedo, as an objective measurement, can be considered a better indicator of grass recovery than subjective interpretations in páramo ecosystems under different land uses.

Credit authorship contribution statement

Conception, design, and supervision of the experiment, PM-D, RC, and GC-R; monitoring and data processing, PM-D; methodology, PM-D, RC, and GC-R; formal analysis, PM-D; writing—original draft preparation, PM-D; visualization, PM-D, and BPW; writing—review and editing, PM-D, RC, BPW, and GC-R. All authors have read and agreed the submitted version of this manuscript.

Declaration of competing interest

The authors declare that they have no competing financial interests or personal relationships that could have influenced the work reported in this paper.

Acknowledgments

This work was funded by the Vice-rectorate for Research of the University of Cuenca https://www.ucuenca.edu.ec/ (Vicerrectorado de Investigación de la Universidad de Cuenca, VIUC), Ecuador, through

Project XVIII–Conc: "Desarrollo de Ecuaciones para la estimación de Evapotranspiración en el Páramo Andino, para condiciones de información hidrometeorológica limitada". We are grateful to the staff and students who contributed to the meteorological monitoring.

Appendix A. Supplementary data

Supplementary data to this article can be found online at https://doi.org/10.1016/j.scitotenv.2022.155010.

References

Arora, V.K., Montenegro, A., 2011. Small temperature benefits provided by realistic afforestation efforts. Nat. Geosci. 4 (8), 514–518. https://doi.org/10.1038/ngeo1182.

Barnes, C.A., Roy, D.P., 2008. Radiative forcing over the conterminous United States due to contemporary land cover land use albedo change. Geophys. Res. Lett. 35 (9), L09706. https://doi.org/10.1029/2008GL033567.

te Beest, M., Sitters, J., Ménard, C.B., Olofsson, J., 2016. Reindeer grazing increases summer albedo by reducing shrub abundance in Arctic tundra. Environ. Res. Lett. 11 (12), 125013. https://doi.org/10.1088/1748-9326/aa5128.

Berrones, G., Crespo, P., Wilcox, B.P., Tobón, C., Célleri, R., 2021. Assessment of fog gauges and their effectiveness in quantifying fog in the Andean páramo. Ecohydrology 14 (6). https://doi.org/10.1002/eco.2300.

Betts, R., 2001. Biogeophysical impacts of land use on present-day climate: near-surface temperature change and radiative forcing. Atmos. Sci. Lett. 2 (1–4), 39–51. https://doi.org/10.1006/asle.2001.0023.

Bozzi, E., Genesio, L., Toscano, P., Pieri, M., Miglietta, F., 2015. Mimicking biochar-albedo feedback in complex Mediterranean agricultural landscapes. Environ. Res. Lett. 10 (8), 084014. https://doi.org/10.1088/1748-9326/10/8/084014.

Bramer, I., Anderson, B.J., Bennie, J., Bladon, A.J., De Frenne, P., Hemming, D., Hill, R.A., Kearney, M.R., Körner, C., Korstjens, A.H., Lenoir, J., Maclean, I.M.D., Marsh, C.D., Morecroft, M.D., Ohlemüller, R., Slater, H.D., Suggitt, A.J., Zellweger, F., Gillingham, P.K., 2018. Advances in monitoring and modelling climate at ecologically relevant scales. Advances in Ecological Research. vol. 58, pp. 101–161. https://doi.org/10.1016/bs.aecr.2017.12.005.

Bright, R.M., Zhao, K., Jackson, R.B., Cherubini, F., 2015. Quantifying surface albedo and other direct biogeophysical climate forcings of forestry activities. Glob. Chang. Biol. 21 (9), 3246–3266. https://doi.org/10.1111/gcb.12951.

Capdevila, P., Stott, I., Beger, M., Salguero-gómez, R., 2020. Towards a comparative framework of demographic resilience. Trends Ecol. Evol. 1–11. https://doi.org/10.1016/j.tree.2020.05.001.

Carrillo-Rojas, G., 2019. On the multi-scale analysis of land-surface mass and energy exchanges for the tropical Andean páramo of Southern Ecuador. Philipps Universitat Marburg.

Carrillo-Rojas, G., Silva, B., Córdova, M., Célleri, R., Bendix, J., 2016. Dynamic mapping of evapotranspiration using an energy balance-based model over an Andean páramo catchment of Southern Ecuador. Remote Sens. 8 (2). https://doi.org/10.3390/rs8020160.

Carrillo-Rojas, G., Silva, B., Rollenbeck, R., Célleri, R., Bendix, J., 2019. The breathing of the Andean Highlands: net ecosystem exchange and evapotranspiration over the páramo of southern Ecuador. Agric. For. Meteorol. 265, 30–47. https://doi.org/10.1016/j.agrformet.2018.11.006.

Carrillo-Rojas, Galo, Schulz, H.M., Orellana-Alvear, J., Ochoa-Sánchez, A., Trachte, K., Célleri, R., Bendix, J., 2020. Atmosphere-surface fluxes modeling for the High Andes: the case of páramo catchments of Ecuador. Sci. Total Environ. 704, 135372. https://doi.org/10.1016/j.scitotenv.2019.135372.

Celleri, R., Willems, P., Buytaert, W., Feyen, J., 2007. Space–time rainfall variability in the Paute basin,Ecuadorian Andes. Hydrol. Process. 21 (24), 3316–3327. https://doi.org/10.1002/hyp.6575.

Chou, S., Chen, B., Chen, J., Wang, M., Wang, S., Croft, H., Shi, Q., 2020. Estimation of leaf photosynthetic capacity from the photochemical reflectance index and leaf pigments. Ecol. Indic. 110 (April 2019), 105867. https://doi.org/10.1016/j.ecolind.2019.105867.

Claussen, M., Brovkin, V., Ganopolski, A., 2001. Biogeophysical versus biogeochemical feedbacks of large-scale land cover change. Geophys. Res. Lett. 28 (6), 1011–1014. https://doi.org/10.1029/2000GL012471.

Correa, A., Ochoa-Tocachi, B., Birkel, C., Ochoa-Sánchez, A., Zogheib, C., Tovar, C., Buytaert, W., 2020. A concerted research effort to advance the hydrological understanding of tropical páramos. Hydrol. Process. 34 (24), 4609–4627. https://doi.org/10.1002/hyp.13904.

Davin, E.L., de Noblet-Ducoudré, N., Friedlingstein, P., 2007. Impact of land cover change on surface climate: relevance of the radiative forcing concept. Geophys. Res. Lett. 34 (13), n/a-n/a. https://doi.org/10.1029/2007GL029678.

Dickinson, R.E., Hanson, B., 1979. Vegetation-Albedo Feedbacks. 29.

Fernandez Monteiro, J.A., Hiltbrunner, E., Körner, C., 2011. Functional morphology and microclimate of Festuca orthophylla, the dominant tall tussock grass in the Andean Altiplano. Flora - Morphology, Distribution, Functional Ecology of Plants. 206(4), pp. 387–396. https://doi.org/10.1016/j.flora.2011.01.001.

Findell, K.L., Shevliakova, E., Milly, P.C.D., Stouffer, R.J., 2007. Modeled impact of anthropogenic land cover change on climate. J. Clim. 20 (14), 3621–3634. https://doi.org/10.1175/JCLI4185.1.

Fletcher, C.G., Thackeray, C.W., Burgers, T.M., 2015. Evaluating biases in simulated snow albedo feedback in two generations of climate models. J. Geophys. Res. Atmos. 120 (1), 12–26. https://doi.org/10.1002/2014JD022546.

Gang, C., Pan, S., Tian, H., Wang, Z., Xu, R., Bian, Z., Pan, N., Yao, Y., Shi, H., 2020. Satellite observations of forest resilience to hurricanes along the northern Gulf of Mexico. For. Ecol. Manag. 472 (March), 118243. https://doi.org/10.1016/j.foreco.2020.118243.

Gong Li, S., Harazono, Y., Oikawa, T., Zhao, H.L., Ying He, Z., Chang, X.L., 2000. Grassland desertification by grazing and the resulting micrometeorological changes in Inner Mongolia. Agric. For. Meteorol. 102 (2–3), 125–137. https://doi.org/10.1016/S0168-1923(00)00101-5.

Guillaume, T., Maranguit, D., Murtilaksono, K., Kuzyakov, Y., 2016. Sensitivity and resistance of soil fertility indicators to land-use changes: new concept and examples from conversion of Indonesian rainforest to plantations. Ecol. Indic. 67, 49–57. https://doi.org/10.1016/j.ecolind.2016.02.039.

Hofstede, R., 1995. The effects of grazing and burning on soil and plant nutrient. Plant Soil 173 (1), 132.

Ingrisch, J., Bahn, M., 2018. Towards a comparable quantification of resilience. Trends Ecol. Evol. 33 (4), 251–259. https://doi.org/10.1016/j.tree.2018.01.013.

IPCC, 2018. In: Masson-Delmotte, V.P. Zhai, Pörtner, H.O., Roberts, D., Skea, J., Shukla, P.R., Pirani, A., Moufouma-Okia, W., Péan, C., Pidcock, R., Connors, S., Matthews, J.B.R., Chen, Y., Zhou, X., Gomis, M.I., Lonnoy, E., Maycock, T., Tignor, M., Waterfield, T. (Eds.), Global warming of 1.5°C. An IPCC special report on the impacts of global warming of 1.5°C above pre-industrial levels and related global greenhouse gas emission pathways, in the context of strengthening the global response to the threat of climate change. IPCC https://doi.org/10.1038/291285a0 In Press.

Lazo, P.X., Mosquera, G.M., McDonnell, J.J., Crespo, P., 2019. The role of vegetation, soils, and precipitation on water storage and hydrological services in Andean Páramo catchments. J. Hydrol. 572, 805–819. https://doi.org/10.1016/j.jhydrol.2019.03.050.

Lukeš, P., Stenberg, P., Mõttus, M., Manninen, T., Rautiainen, M., 2016. Multidecadal analysis of forest growth and albedo in boreal Finland. Int. J. Appl. Earth Obs. Geoinf. 52, 296–305. https://doi.org/10.1016/j.jag.2016.07.001.

MAATE, 2015. Ministery of Environment Water and Ecological Transition. https://www.ambiente.gob.ec/.

Marín, F., Dahik, C., Mosquera, G., Feyen, J., Cisneros, P., Crespo, P., 2018. Changes in soil hydro-physical properties and SOM due to pine afforestation and grazing in andean environments cannot be generalized. Forests 10 (1), 17. https://doi.org/10.3390/f10010017.

Montenegro-Díaz, P., Ochoa-Sánchez, A., Célleri, R., 2019. Impact of tussock grasses removal on soil water content dynamics of a tropical mountain hillslope. Ecohydrology 12 (8), 1–12. https://doi.org/10.1002/eco.2146.

Mosquera, G.M., Lazo, P.X., Célleri, R., Wilcox, B.P., Crespo, P., 2015. Runoff from tropical alpine grasslands increases with areal extent of wetlands. Catena 125, 120–128. https://doi.org/10.1016/j.catena.2014.10.010.

Ochoa-Sánchez, A.E., Crespo, P., Carrillo-Rojas, G., Marín, F., Célleri, R., 2020. Unravelling evapotranspiration controls and components in tropical Andean tussock grasslands. Hydrol. Process. 34 (9), 2117–2127. https://doi.org/10.1002/hyp.13716.

Orwin, K.H., Wardle, D.A., 2004. New indices for quantifying the resistance and resilience of soil biota to exogenous disturbances. Soil Biol. Biochem. 36 (11), 1907–1912. https://doi.org/10.1016/j.soilbio.2004.04.036.

Padrón, R.S., Wilcox, B.P., Crespo, P., Célleri, R., 2015. Rainfall in the Andean páramo: new insights from high-resolution monitoring in Southern Ecuador. J. Hydrometeorol. 16 (3), 985–996. https://doi.org/10.1175/JHM-D-14-0135.1.

Pielke, R.A., Marland, G., Betts, R.A., Chase, T.N., Eastman, J.L., Niles, J.O., Niyogi, D.D.S., Running, S.W., 2002. The influence of land-use change and landscape dynamics on the climate system: relevance to climate-change policy beyond the radiative effect of greenhouse gases. Philos. Trans. R. Soc. London, Ser. A 360 (1797), 1705–1719. https://doi.org/10.1098/rsta.2002.1027.

Podwojewski, P., Poulenard, J., Zambrana, T., Hofstede, R., 2006. Overgrazing effects on vegetation cover and properties of volcanic ash soil in the páramo of llangahua and La Esperanza (Tungurahua, Ecuador). Soil Use Manag. 18 (1), 45–55. https://doi.org/10.1111/j.1475-2743.2002.tb00049.x.

Postigo, J.C., 2014. Perception and resilience of Andean populations facing climate change. J. Ethnobiol. 34 (3), 383–400. https://doi.org/10.2993/0278-0771-34.3.383.

Richardson, A.D., Keenan, T.F., Migliavacca, M., Ryu, Y., Sonnentag, O., Toomey, M., 2013. Climate change, phenology, and phenological control of vegetation feedbacks to the climate system. Agric. For. Meteorol. 169, 156–173. https://doi.org/10.1016/j.agrformet.2012.09.012.

Rosset, M., Montani, M., Tanner, M., Fuhrer, J., 2001. Effects of abandonment on the energy balance and evapotranspiration of wet subalpine grassland. Agric. Ecosyst. Environ. 86 (3), 277–286. https://doi.org/10.1016/S0167-8809(00)00290-5.

Sagan, C., Toon, O., Pollack, J., 1979. Anthropogenic albedo changes and the Earth's climate. Science 206 (4425), 1363–1368.

SENPLADES, 2017. Plan Nacional de Desarrollo 2017-2021. Toda una vida. SENPLADES.

Sucozhañay, A., Célleri, R., 2018. Impact of rain gauges distribution on the runoff simulation of a small mountain catchment in Southern Ecuador. Water 10 (9), 1169. https://doi.org/10.3390/w10091169.

Teng, Y., Zhan, J., Agyemang, F.B., Sun, Y., 2020. The effects of degradation on alpine grassland resilience: a study based on meta-analysis data. Glob. Ecol. Conserv. 24, e01336. https://doi.org/10.1016/j.gecco.2020.e01336.

VanCuren, R., 2012. The radiative forcing benefits of "cool roof" construction in California: quantifying the climate impacts of building albedo modification. Clim. Chang. 112 (3–4), 1071–1083. https://doi.org/10.1007/s10584-011-0250-2.

Wang, X., Huang, Z., Hong, M.M., Zhao, Y.F., Ou, Y.S., Zhang, J., 2019. A comparison of the effects of natural vegetation regrowth with a plantation scheme on soil structure in a geological hazard-prone region. Eur. J. Soil Sci. 70 (3), 674–685. https://doi.org/10.1111/ejss.12781.

de Wit, H.A., Bryn, A., Hofgaard, A., Karstensen, J., Kvalevåg, M.M., Peters, G.P., 2014. Climate warming feedback from mountain birch forest expansion: reduced albedo dominates carbon uptake. Glob. Chang. Biol. 20 (7), 2344–2355. https://doi.org/10.1111/gcb.12483.

Xiao, L., Che, T., Chen, L., Xie, H., Dai, L., 2017. Quantifying snow albedo radiative forcing and its feedback during 2003–2016. Remote Sens. 9 (9), 883. https://doi.org/10.3390/rs9090883.

Zhao, W., Hu, Z., Li, S., Guo, Q., Liu, Z., Zhang, L., 2017. Comparison of surface energy budgets and feedbacks to microclimate among different land use types in an agro-pastoral ecotone of Northern China. Sci. Total Environ. 599–600, 891–898. https://doi.org/10.1016/j.scitotenv.2017.04.200.

Zheng, L., Zhao, G., Dong, J., Ge, Q., Tao, J., Zhang, X., Qi, Y., Doughty, R.B., Xiao, X., 2019. Spatial, temporal, and spectral variations in albedo due to vegetation changes in China's grasslands. ISPRS J. Photogramm. Remote Sens. 152, 1–12. https://doi.org/10.1016/j.isprsjprs.2019.03.020.